

Lawrence Berkeley National Laboratory

Recent Work

Title

ARGONNE NATIONAL LABORATORY HVEM SUMMER INSTITUTE LECTURE - KINETICS II

Permalink

<https://escholarship.org/uc/item/1hz1x4dp>

Author

Westmacott, K.H.

Publication Date

1982-08-01

c.d



Lawrence Berkeley Laboratory

UNIVERSITY OF CALIFORNIA

RECEIVED
LAWRENCE
BERKELEY LABORATORY

Materials & Molecular Research Division

NOV 16 1982

LIBRARY AND
DOCUMENTS SECTION

Presented at the HVEM Summer Institute Workshop,
Argonne National Laboratory, Argonne, IL,
July 21-23, 1982

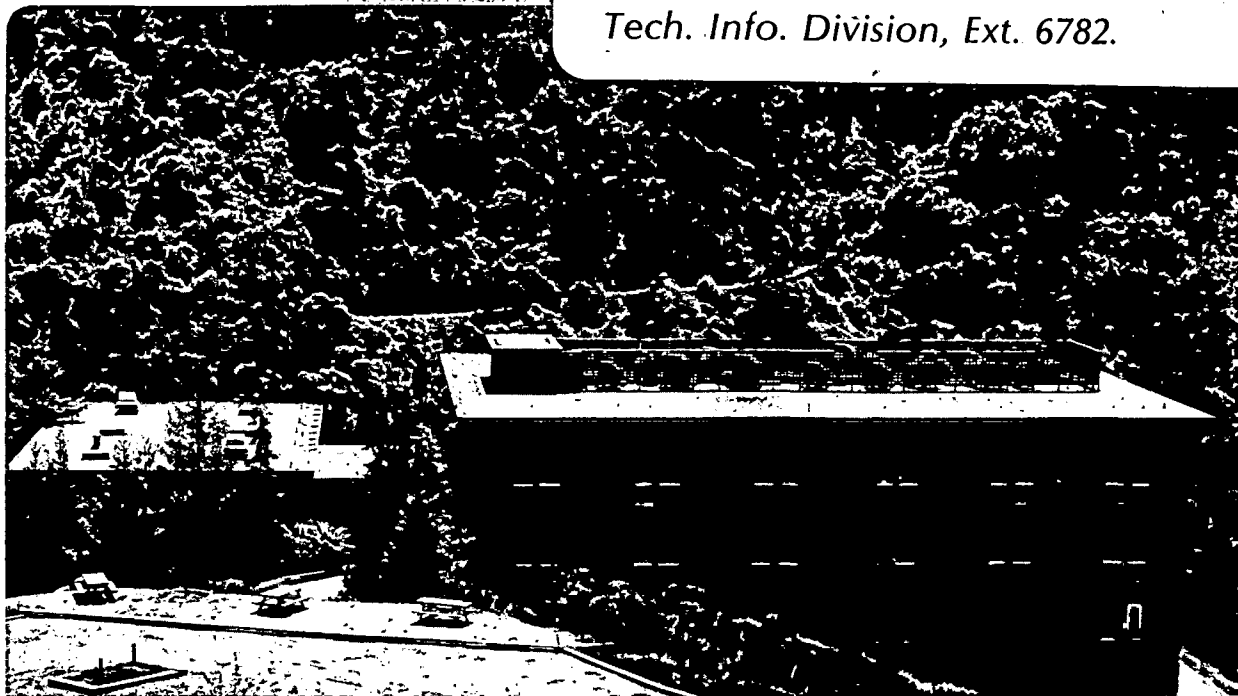
ARGONNE NATIONAL LABORATORY HVEM SUMMER INSTITUTE
LECTURE - KINETICS II

K.H. Westmacott

August 1982

TWO-WEEK LOAN COPY

*This is a Library Circulating Copy
which may be borrowed for two weeks.
For a personal retention copy, call
Tech. Info. Division, Ext. 6782.*



LBL-14720
c.d

DISCLAIMER

This document was prepared as an account of work sponsored by the United States Government. While this document is believed to contain correct information, neither the United States Government nor any agency thereof, nor the Regents of the University of California, nor any of their employees, makes any warranty, express or implied, or assumes any legal responsibility for the accuracy, completeness, or usefulness of any information, apparatus, product, or process disclosed, or represents that its use would not infringe privately owned rights. Reference herein to any specific commercial product, process, or service by its trade name, trademark, manufacturer, or otherwise, does not necessarily constitute or imply its endorsement, recommendation, or favoring by the United States Government or any agency thereof, or the Regents of the University of California. The views and opinions of authors expressed herein do not necessarily state or reflect those of the United States Government or any agency thereof or the Regents of the University of California.

Argonne National Laboratory

HVEM Summer Institute Lecture - Kinetics II

K. H. Westmacott

National Center for Electron Microscopy
Materials and Molecular Research Division
Lawrence Berkeley Laboratory
University of California
Berkeley, CA 94720

August 1982

This work was supported by the Director, Office of Energy Research,
Office of Basic Energy Sciences, Division of Materials Science of
the U.S. Department of Energy under Contract No. DE-AC03-76SF00098.

Argonne National Laboratory HVEM Summer Institute Lecture - Kinetics II

K. H. Westmacott
National Center for Electron Microscopy
Materials and Molecular Research Division
Lawrence Berkeley Laboratory
Berkeley, California 94720

Introduction

Before the advent of transmission electron microscopy, the early stages of solid state phase transformations, such as precipitation processes, could be studied only indirectly. Changes in the fine scale microstructure were inferred by studying corresponding changes in a bulk structure-sensitive property such as electrical resistivity, internal friction, or x-ray diffraction patterns. Because these changes occurred at levels beyond the resolution capability of optical microscopy, this stage was originally termed pre-precipitation.

The application of thin foil TEM to this problem has several advantages that were immediately recognised and exploited. (1) The entire precipitation sequence, from the initial decomposition of the supersaturated solid solution to the formation of the final equilibrium phase, can be followed. (2) The various intermediate phase habit planes, morphologies and interphase interface structures may be directly characterized and related to the precipitate and matrix structure through parallel selected area diffraction studies. (3) The capability to perform in-situ dynamic studies of precipitate growth, transition, and dissolution processes became possible. This technique allows the behavior of individual particles to be observed in contrast to studies on bulk crystals where only average properties are measured. In the first experiments of this type, Thomas and Whelan, 1961, studied the growth and dissolution of precipitates in Al-4% Cu and deduced solute diffusion coefficients from the observed shrinkage curves. Later, Hren and Thomas, 1963, studied the growth of γ' in Al-Ag and showed for the first time the role of dislocations in precipitate nucleation.

Since this time a number of other studies have been conducted (see recent excellent reviews by Butler, 1979 and Butler and Hale, 1981) but the full potential of the technique has still not been exploited.

The purpose of this contribution is to focus on some of the important metallurgical parameters that can be determined from precise in-situ measurements, and to emphasize the role HVEMs can play in research of this type.

2. Experimental Methods

The reader is referred to the text by Butler and Hale for a comprehensive treatise on the techniques and methods available for optimizing HVEM utilization for in-situ studies. Here only a few cautionary notes and tips for improving experimental measurements during hot-stage experiments are offered.

(1) Effects of Radiation Damage

High voltage electron microscopy for in-situ dynamic studies is a double-edged sword; while the increased voltage allows one to study much thicker foils than at 100kV, the onset of displacement damage above the voltage threshold, E_T , for production of Frenkel pairs can lead to complications which can go unsuspected or unrecognized. Fortunately, the perturbing effects of this radiation damage are most significant at temperatures where the point defect mobilities are low, whereas studies of secondary defect or precipitate shrinkage kinetics are, by their nature, conducted at temperatures where mobilities are high.

At higher temperatures the concentration of vacancies in thermal equilibrium in the crystal increases and eventually, at a temperature T_c , the radiation-induced defect concentrations are no longer dominant. These effects have been quantified, see for example Makin and Sharp (1968), Bricknell and Edington (1977), and the procedure for calculating T_c explained. Values of T_c for a number of metals are given in Table I (due to Bricknell and Edington).

TABLE I

Critical temperatures for a number of elements at which the thermal vacancy concentration equals that produced by 1 MV electron irradiation with a beam current of 0.1 A.cm²

Element	T_c (°C)	Element	T_c (°C)	Element	T_c (°C)
Aluminium	260	Magnesium	270	Titanium	720
Copper	490	Nickel	820	Zinc	110
Iron	810	Lead	130	Zirconium	780

In spite of this disadvantage the HVEMs penetration advantage is still indispensable for studying large scale structures in any material, structures in materials with high atomic number, and hard to thin materials such as glasses, minerals and some ceramics. In addition, several steps may be taken to eliminate or minimize the effects of radiation damage. These are (1) the obvious one, operate the microscope below E_T . (2) set up imaging conditions, i.e. diffraction conditions, focussing etc., in an area A adjacent to the primary area B to be studied and limit electron exposure of B to that required for periodic image recording. In this way a comparison of areas A and B will reveal any effects of radiation damage. (3) use an image intensifier and record images on a video cassette. This can be carried out at very low primary electron beam fluxes.

(2) Effect of Environment

In a hot stage experiment the possible effects of the specimen environment on the results should always be borne in mind. Refractory metals are particularly susceptible to contamination by reaction with residual gases in the microscope vacuum and special precaution and modifications to the microscope to improve the vacuum are necessary for this type of study (see e.g. Regnier et al. 1977). Nonetheless the larger specimen chamber and greater pumping access to the specimen area possible with the HVEM are still an advantage. Furthermore, the use of an environmental, or gas reaction, cell in the HVEM, in principle, allows one to exercise a close control over the specimen environment during a heating experiment. Unfortunately, this is usually achieved at the expense of another important function such as additional axis of tilt. The contribution by E. Kenik to this workshop will describe in detail the experiments possible with an environmental cell.

(3) Optimizing Imaging Conditions

Under favorable conditions (e.g. the availability of a double-tilt heating stage with good temperature control and small thermal drift rate) and with patience, experimental shrinkage curves for dissolving secondary defect and precipitates can be obtained to quite high accuracy. As is well known the optimum imaging conditions at high voltages are different to those at 100kV and 2-beam conditions are obtained only for high order reflections. In many cases this is satisfactory, but it is often advantageous to employ special imaging conditions to

improve the quality of the data further. For example, it has been shown recently (Dahmen and Westmacott, 1982) that in many alloy systems the initial nucleation and subsequent growth of precipitates occurs semicoherently. That is, the precipitate plates and growth ledges are bounded by dislocations. In these systems sharper, better defined, images of the precipitate boundaries may be obtained either by using the weak beam dark field technique or high order bright field imaging. The measurement of precipitate diameters during dissolution is then facilitated.

In some cases the presence of a high density of precipitates of different variants leads to some confusion of the micrograph due to image overlap. This problem can be circumvented by forming a dark field image using a precipitate diffraction spot arising from only one of the variants. Again, in the HVEM a high quality image can be obtained simply by placing the objective aperture over the off-optical axis beam (i.e. no beam tilting is required).

(4) Stereomicroscopy

An alternative technique for reducing image overlap in a thick foil is to record stereo-pairs of micrographs. While this is somewhat more time-consuming and demanding on the experimenter, it can be done if the shrinkage rate is not too fast, and considerable advantages can accrue. For example, the observation of atypical, anomolous kinetics might, during subsequent examination of the micrographs in a stereoviewer, be related to the nearby presence of a free surface, grain boundary, or lattice defect, or to the overlapping of diffusion fields of other defects.

It is also found that in thick foils precipitate coarsening typical of bulk behavior may be observed. Although it has not yet been attempted, this suggests that by observing the structures over a long time and employing the sophisticated computerized stereo-techniques developed by L. Thomas et al., 1970, 1974, Ostwald ripening processes might be followed directly on individual particles.

3. Practical Examples

In this section some selected examples of experiments that have been or could be done are outlined with emphasis on the quantitative parameters derivable from the kinetics analysis. It should be pointed out that in some cases to improve the temperature control the annealing treatments were performed ex-situ and the specimen returned to the microscope periodically. However, the availability of improved hot stages (Makin 1974) now makes this procedure unnecessary.

The underlying assumptions are (i) that the foil surfaces are the principal sinks for the diffusing species and defects are sufficiently widely spaced that there is no interaction between their diffusion fields (this is represented schematically in Fig. 1), (ii) that the foil surfaces are perfect sinks for vacancies, and (iii) that the defect shrinkage rate is diffusion rather than emission controlled. With the use of Fick's Law, this allows the boundary conditions for the diffusion equation to be defined and an expression for the shrinkage rate to be derived.

(i) Dislocation Loop Shrinkage and the Measurement of γ_I .

The first experiments of this type were performed on quenched-in vacancy loops by Silcox and Whelan 1960, but Smallman and coworkers 1967, refined the techniques to the point where accurate measurements of stacking fault energies γ_{SF} is possible in metals where γ_{SF} is $> \sim 100 \text{ mJ/m}^2$.

If the experiments are performed on large faulted dislocations loops, the diffusion equation is solved for cylindrical symmetry and the stacking fault energy provides the dominant driving force for shrinkage in the temperature range where self-diffusion becomes rapid.

The general rate equation governing shrinkage,

$$\frac{dr}{dt} = \frac{-2\pi D}{b \ln(t/b)} \left[\exp\left(\frac{(dE/dn)B^2}{kT}\right) - 1 \right] \quad (1)$$

where D is the self diffusion coefficient, dE/dn is the climb force acting on the defect causing it to shrink, and B^2 is the area of a vacancy in the loop plane, becomes

$$\left(\frac{dr}{dt}\right)_F = \frac{-2\pi D}{b \ln(t/b)} \left[\exp\left(\frac{\gamma_I B^2}{kT}\right) - 1 \right] \quad (2)$$

where γ_I is the intrinsic stacking fault energy.

Smallman et al. compared the shrinkage rate of imperfect (faulted) and perfect prismatic loops to eliminate D from Eq. 2 and obtain γ_I .

(ii) Measurements of the Activation Energies for Self Diffusion, Q_{SD} .

It was pointed out by Peck and Westmacott, 1971, that since γ_I is insensitive to small changes in temperature, Eq. 2 could be used to measure Q_{SD} in systems where γ_I is known. Furthermore, it was shown that particularly accurate values

could be obtained by studying large loops which allowed the shrinkage rate to be established at two different temperatures on the same loop. In this way variations in the shrinkage rates due to the different positions and geometries of the loops in the foil could be cancelled.

Experimental data from this type of study in aluminum are given in Figs. 2 and 3. The micrographs showing regular loop shrinkage in Fig. 2 and the graph obtained by plotting the loop radius against annealing time at 150°C and 100°C confirms the linear shrinkage predicted by integration of Eq. 2.

Since the factor in the square brackets can be computed at each temperature, the ratio of the rates at 150°C and 100°C allows the required activation energy to be obtained directly viz:

$$\dot{(r_1)}_F / \dot{(r_2)}_F = A \exp \frac{Q_{SD}}{k} \left(\frac{1}{T_2} - \frac{1}{T_1} \right) \quad (3)$$

where A is a small correction factor.

Using this technique a value of $Q_{SD} = 1.19\text{eV}$ was obtained for very pure aluminum. This is significantly lower than the traditionally accepted value derived from radioactive tracer measurements (1.48eV) but in good accord with more recent positron annihilation determinations.

(iii) Measurements of Surface Energy γ_S

Since the majority of the energy of a void or cavity in a metal resides in its internal surfaces, measurements of void shrinkage kinetics allow a direct estimate of γ_S to be made. The procedure is again to produce large defects by quenching or irradiation and record the shrinkage during isothermal annealing. This is particularly advantageous in the case of surface energy since the difficulty of keeping the surfaces uncontaminated encountered in conventional experiments is circumvented.

In the case of void shrinkage, the diffusion geometry is spherical and Eq. (1) becomes

$$\left(\frac{dr}{dt} \right)_V = -\frac{D}{r} \left[\exp \left(\frac{2\Omega\gamma_S}{rkT} \right) - 1 \right] \quad (4)$$

where Ω is the atomic volume.

For large voids ($r > 500\text{\AA}$) the exponential term can be approximated to the first two terms of the series expansion and Eq. (4) may then be integrated to give

$$r_0^3 - r^3 = \left(\frac{6D\Omega\gamma_S}{kT} \right) t \quad (5)$$

Void shrinkage kinetics were studied in aluminum and copper by Westmacott et al. 1968 and Johnston et al., 1969 respectively. By comparing the observed shrinkage rates with those for dislocation loops, D was eliminated and values for $\gamma_S^{\text{Al}} = 1140\text{mJ/m}^2$ and $\gamma_S^{\text{Cu}} = 2600\text{mJ/m}^2$ were found. Volin and Balluffi 1968 used void shrinkage measurements in Al to estimate D_{SD} in the temperature range 85 - 209°C.

In an interesting variation on these experiments Volin and Balluffi, 1968, and Westmacott and Smallman, 1969/70 compared the rate of shrinkage of voids in the matrix with that of voids threaded by a dislocation to the foil surfaces in order to study dislocation pipe diffusion.

In the former case the voids were produced by quenching and a large increase in the shrinkage rate was observed due to diffusion of vacancies down the dislocation core. In the latter experiments the voids were introduced by neutrons in the presence of gas. Under these circumstances no enhancement by the dislocations was observed indicating that the voids contained significant amounts of gas and that the shrinkage was no longer diffusion-controlled.

(iv) Precipitate Growth Studies

The most difficult kinetic studies to perform and interpret, but potentially the most rewarding are those on precipitate structures. The difficulties arise from the fact that unlike secondary defects (dislocation loops or voids), in most cases the driving forces for precipitate dissolution, the interfacial energy γ_{IF} , can only be guessed, and the solute concentrations at the boundary conditions needed to solve the diffusion equation are also not so readily established.

Development of the equations governing the shrinkage or coarsening of spherical precipitate particles is completely analogous to that for voids. Because the driving force is smaller ($\gamma_{IF} \ll \gamma_S$), however, the solute concentration in equilibrium with the particle is smaller and the question of whether the shrinkage process is diffusion- or interface-controlled cannot be answered a priori. Fortunately, differences in the form of the two equations allows a distinction to be made when experimental data is available.

For the diffusion-controlled case the rate equation in its simplest formulation given by Greenwood, 1968, is

$$\frac{dr}{dt} = - \frac{D}{r} (S_r - S_a) \quad (6)$$

where S_r is the solute concentration in equilibrium with a particle of radius r , and S_a the average solute concentration a long distance from the particle.

If the rate controlling step is passage of material across the particle/matrix interface

$$\frac{dr}{dt} = - C(S_r - S_a)$$

where C is a constant. This equation is appropriate for the case where $D \gg Cr$.

After further substitution and rearrangement Eq. 6 becomes

$$\frac{dr}{dt} = \frac{2DS\gamma_{IF}}{kT r} \left(\frac{1}{\bar{r}} - \frac{1}{r} \right) \quad (7)$$

where \bar{r} is the arithmetic mean radius of the particles in the system and S is the solubility of a particle of infinite radius.

The corresponding equation for the interface-controlled case is

$$\frac{dr}{dt} = \frac{2C\gamma_{IF}\Omega S}{kT} \left[\frac{\sum r_i}{\sum r_i^2} - \frac{1}{r} \right]$$

where r_i is the radius of the i^{th} particle.

In the Lifshitz-Slyozov, 1961, and Wagner, 1961 the equation is given in terms of the average particle radius and is applied to data obtained from Ostwald ripening experiments, then

$$\bar{r}^3 - \bar{r}_0^3 = Kt \quad (8)$$

where \bar{r}_0 is the average particle radius at the outset, the average radius after time t , and $K = 2D\gamma_{IF}/\rho^2 kT$. In this form, the similarity between Eqs. (8) and (5) and (8) and (7) is again evident.

In order to simplify the problems with precipitation processes, it is desirable to work initially on the simplest systems available. In this section the results of some preliminary in-situ observations on precipitate dissolution in a very dilute Pt-C alloy are presented.

From detailed contrast analysis on quenched Pt-C specimens it is known that the initial decomposition of the supersaturated solution results in formation of semicoherent platelets of carbon (designated α) on $\{100\}$ planes. During subsequent aging some of the α precipitates absorb a second layer of vacancies and transform to α' . The α' precipitates are isomorphous with Al_2Cu and have a bct crystal structure and a composition of Pt_2C .

It is instructive to study the shrinkage kinetics of α and α' to compare their stabilities and learn more about the dissolution and growth mechanisms, Westmacott *et al.*, 1982. Fig. 4 shows a shrinkage sequence of α precipitates at $\sim 450^\circ C$ taken in the 1.5MeV HVEM at 900kV. From Fig. 4a-d and the plot of radius vs. time, Fig. 4e, the regular shrinkage behavior is apparent. Since the α precipitates form by the co-precipitation of vacancies and carbon atoms, their dissolution is analogous to faulted loop annealing. This suggests further measurements at different temperatures could give information on vacancy/solute complex diffusion.

It was also interesting to note that while the α precipitates in the thin regions of the foil shrank and disappeared, in thicker regions they remained unchanged (Fig. 5). This indicates careful measurements of these precipitates could provide direct coarsening data on individual particles for comparison with Eq. 7.

In contrast to the α precipitates, the α' required temperatures almost $100^\circ C$ higher for dissolution. Again the shrinkage was regular and constant (Fig. 6) suggesting further measurements will be useful. The higher temperatures reflect the greater stability of the carbide structure. Dissolution could be now interface-controlled and additional analysis may provide values for dissociation energies.

Radiation-Induced Precipitate Dissolution

Another important application of the HVEM is in studies of the stability of precipitate structures in a radiation environment. For example, the detailed experiments on phase stability in Al-Cu during in-situ electron irradiation by Sklad

and Mitchell, 1975, showed striking and interesting structural changes resulted from the enhanced diffusion effects. Recently, similar studies on the Pt-C interstitial system by Regnier et al., 1982, have revealed that complex dissolution processes occur at electron energies far below those required to displace the matrix Pt atoms. Fig. 7 shows the changes that occur in the α plates during exposure in the HVEM at 1MeV (E_T for Pt is ~ 1.3 MeV). Damage in the matrix is attributable to displacement of Pt atoms via secondary collisions with C atoms, and that in the precipitate to primary displacements of the carbon. Thus three different damage regimes may be identified, (i) that where the electron energy is sufficient only to displace the carbon atom from the precipitate ($380 < E < 560$ kV), (ii) that where in addition to (i) the displaced carbon energy is sufficient to displace Pt atoms in secondary collisions ($560 < E < 1300$), (iii) that where in addition to (i) and (ii) the electron energy is sufficient to displace a Pt atom in a direct collision ($E > 1300$). These processes are shown schematically in Fig. 8. It is clear that the HVEM is an indispensable tool in this type of investigation.

Summary

The purpose of this contribution was to outline some of the ways in which the High Voltage Electron Microscope can be used to study the kinetics of secondary defect shrinkage and precipitate particle growth and dissolution. In many cases, good agreement between the predictions of theory and the experimental observations are found and this provides not only insights into the mechanisms underlying the processes, but also quantitative measurement of parameters of metallurgical importance.

To summarize, some of the advantages of the HVEM in kinetic studies: (1) unlike bulk studies where only average behavior is measured, precise measurements on individual particles may be made; (2) in some systems it is useful for rapidly establishing phase boundaries, (3) anomalous behavior such as may occur by interactions with lattice defects and boundaries may be studied (4) growth and dissolution mechanisms may be established, (5) phase stability in an irradiation environment may be studied directly.

It was possible to give only a few examples here, and the reader is referred to the book by Butler and Hale for a detailed treatment of the subject and a comprehensive list of references.

Acknowledgements

This was supported by the Director, Office of Energy Research, Office of Basic Energy Sciences, Division of Materials Science of the U. S. Department of Energy under Contract No. DE-AC03-76SF00098. I wish to thank Drs. P. Regnier and N. Q. Lam for stimulating discussions and Dr. Uli Dahmen for his critical comments on the manuscript.

References

- R. H. Bricknell and J. W. Edington, *Acta Met.* 25, 447 (1977).
- E. P. Butler, *Rep. Prog. Phys.* 42, 833 (1979).
- E. P. Butler and K. Hale, "Dynamic Experiments in the Electron Microscope", (North-Holland: Amsterdam) (1981).
- U. Dahmen, M. J. Witcomb and K. H. Westmacott, submitted to *Acta Met.*
- G. W. Greenwood, *Met. Sci. J.* 2, 1 (1968).
- J. J. Hren and G. Thomas, *Met. Trans.* 227, 308 (1963).
- I. A. Johnston, P. S. Dobson and R. E. Smallman, *Cryst. Latt. Defects* 1, 47 (1969).
- J. M. Lifshitz and V. V. Slyozov, *J. Phys. Chem. Solids* 19, 35 (1961).
- M. J. Makin, *HVEM Conf. (Academic: London)*, p. 365 (1974).
- M. J. Makin and J. V. Sharpe, *J. Mat. Sci.* 3, 360 (1968).
- R. L. Peck and K. H. Westmacott, *Met. Sci. J.* 5, 155 (1971); 9, 283 (1975).
- P. Regnier, N. Q. Lam and K. H. Westmacott, *Scripta Met.* 16, 643 (1982).
- J. Silcox and M. J. Whelan, *Phil. Mag.* 5, 1 (1960).
- P. S. Sklad and T. E. Mitchell, *Acta Met.* 23, 1287 (1975).
- R. E. Smallman, P. S. Dobson and P. J. Goodhew, *Phil. Mag.* 16, 9 (1967).
- G. Thomas and M. J. Whelan, *Phil. Mag.* 6, 1103 (1961).
- L. E. Thomas, L. J. Cuddy and S. Lentz, *EMSA Proceedings*, p. 38 (1970); p. 362 (1974).
- R. Valle, B. Genty, A. Marraud and P. Regnier, *5th Int. Conf. on HVEM, Kyoto* (1977).

T. E. Volin and R. W. Balluffi, Phys. Stat. Sol. 25, 163 (1968).

C. Wagner, Z. Electrochem. 65, 581 (1961).

K. H. Westmacott, U. Dahmen and M. J. Witcomb, submitted to Acta Met. (1982).

K. H. Westmacott, P. S. Dobson and R. E. Smallman, Met. Sci. J. 2, 177 (1968).

K. H. Westmacott and R. E. Smallman, Mat. Sci. and Eng. 5, 325 (1969/70).

Figure Captions

- Fig. 1. Diagram showing cylindrical diffusion geometry for a large defect shrinking in a foil of thickness $2t$. C_x is the vacancy concentration in equilibrium with the defect and C_0 the equilibrium concentration in the matrix.
- Fig. 2. Series of micrographs showing regular shrinkage of faulted dislocation loops in aluminum during isothermal annealing at 150 and 100°C (after Peck).
- Fig. 3. Typical plots of loop radius versus time showing constant shrinkage rates in all cases.
- Fig. 4. Micrograph sequence (a-d) showing regular shrinkage of α plate precipitates in a Pt-C alloy. (Thanks are due to D. Ackland for this series.) The graph (e) shows the plot of radius versus time for the precipitates numbered in (b).
- Fig. 5. α precipitates in Pt-C undergoing coarsening in thick regions of the foil. Under the same annealing conditions (cf. Fig. 4) precipitates in thinner regions shrink and disappear.
- Fig. 6. Shrinkage of α' carbide plate precipitates during isothermal annealing at 788K. [Fig. 6e is the corresponding shrinkage plot showing linear behavior.]
- Fig. 7. Sequence showing the progressive dissolution of α precipitates during ambient temperature irradiation at 1MeV in the HVEM.
- Fig. 8. Schematic diagram showing the three damage regimes in Pt-C. (i) $380 < E < 560$ keV, carbon atoms undergo primary collisions with the electrons and are displaced from the precipitate. (ii) $560 < E < 1300$ keV Frenkel pairs are formed in the matrix by secondary collisions of carbon with Pt atoms. (iii) $1300 \ll E$ primary collisions between electrons and Pt atoms produce Frenkel defects.

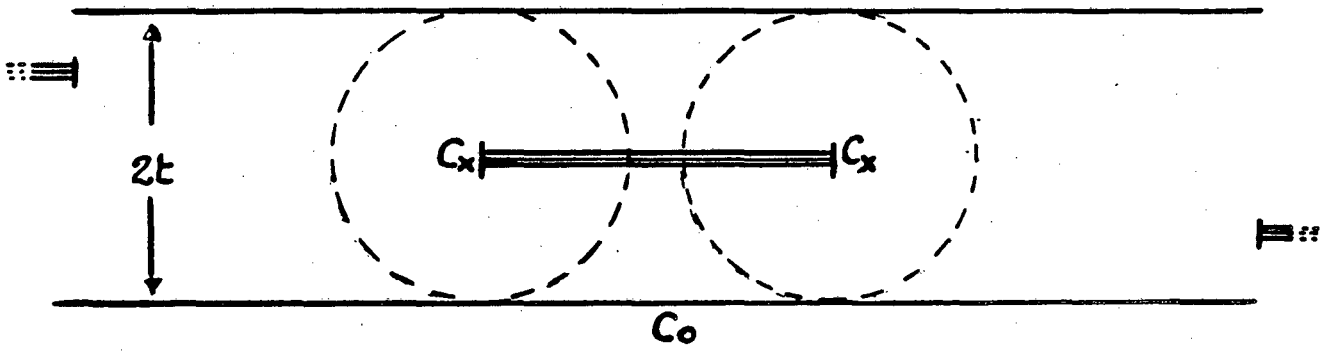
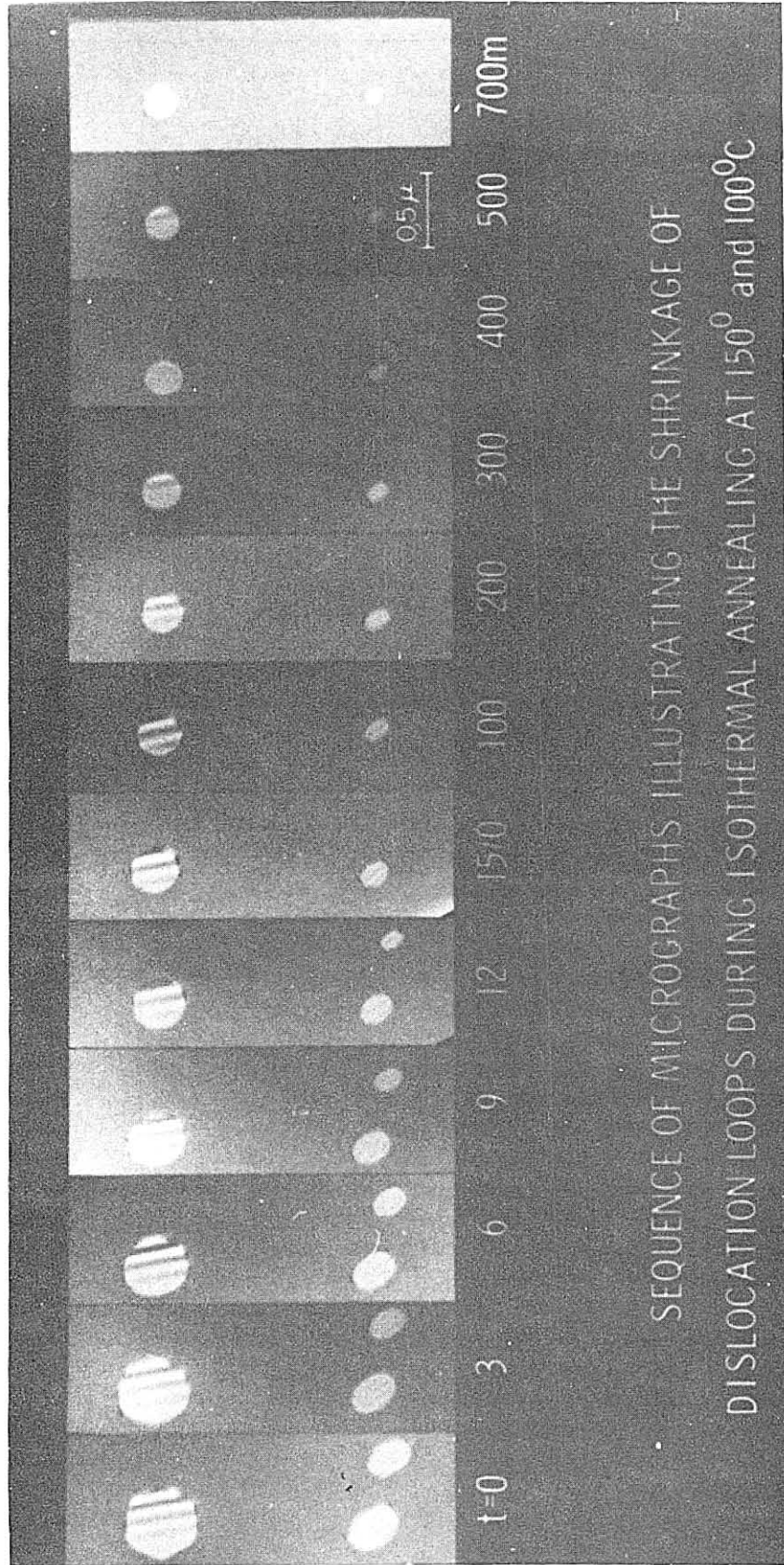


Fig. 1

7
8



SEQUENCE OF MICROGRAPHS ILLUSTRATING THE SHRINKAGE OF DISLOCATION LOOPS DURING ISOTHERMAL ANNEALING AT 150° and 100°C

XBB 828-7481

Fig. 2

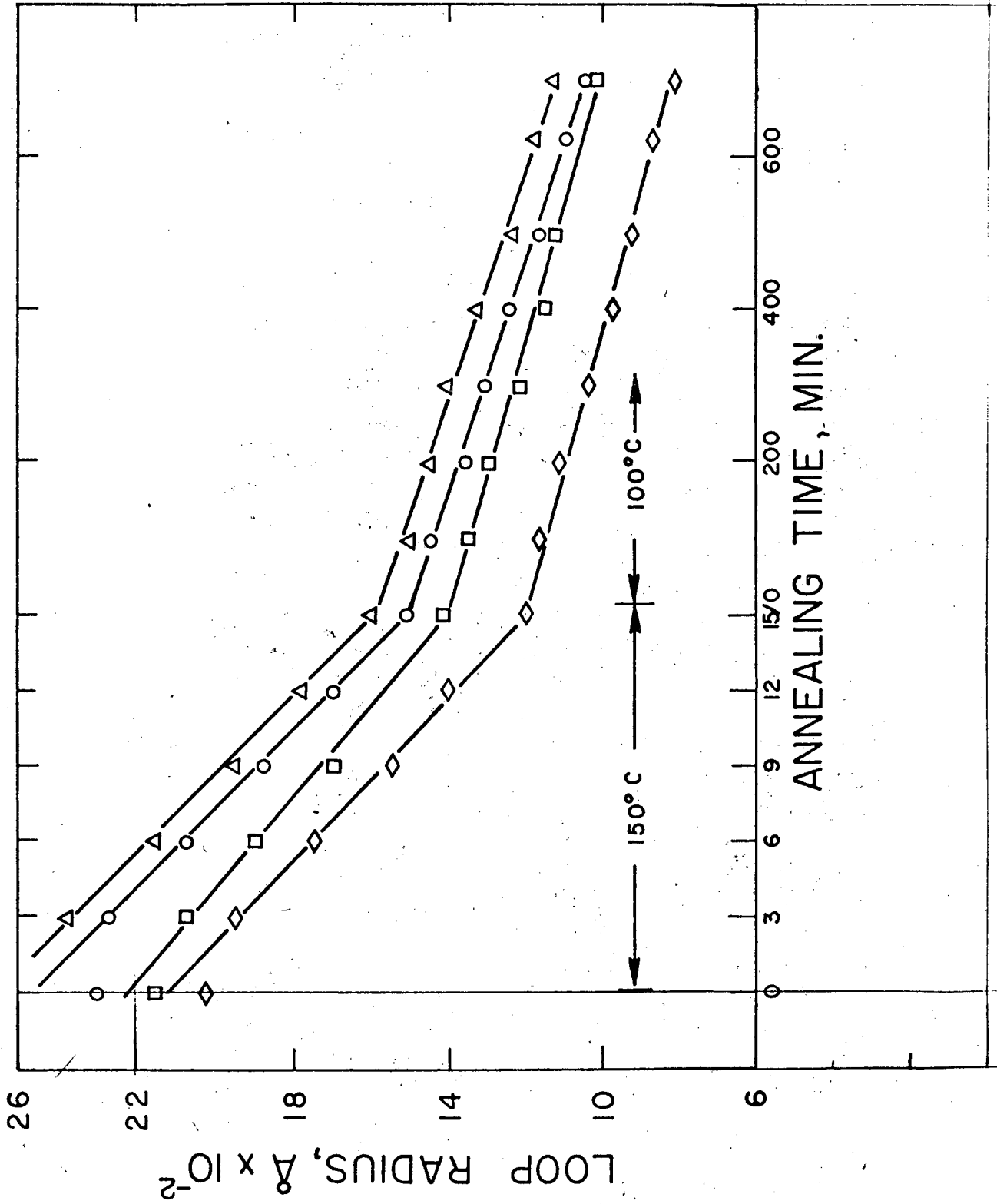


Fig. 3

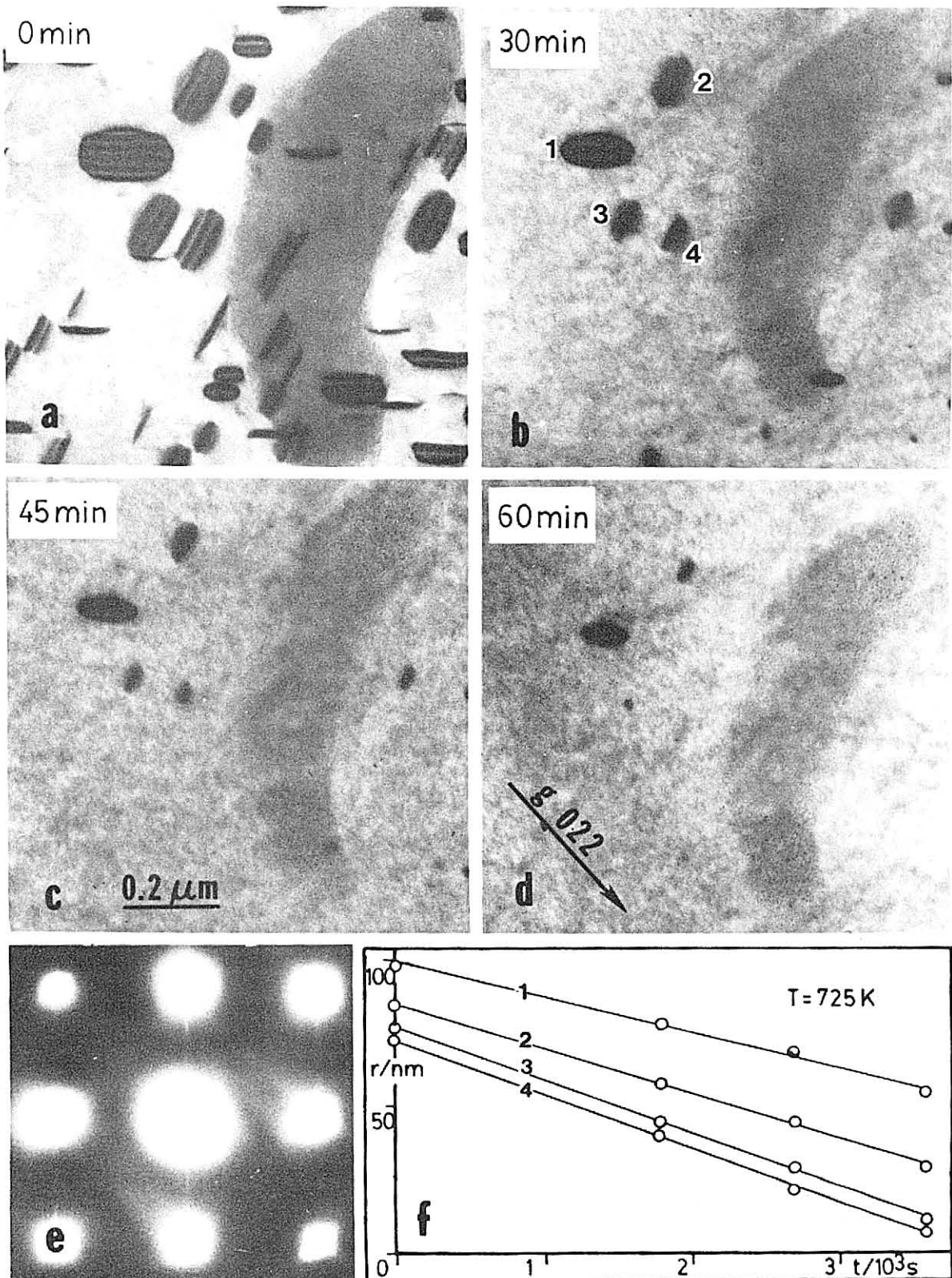
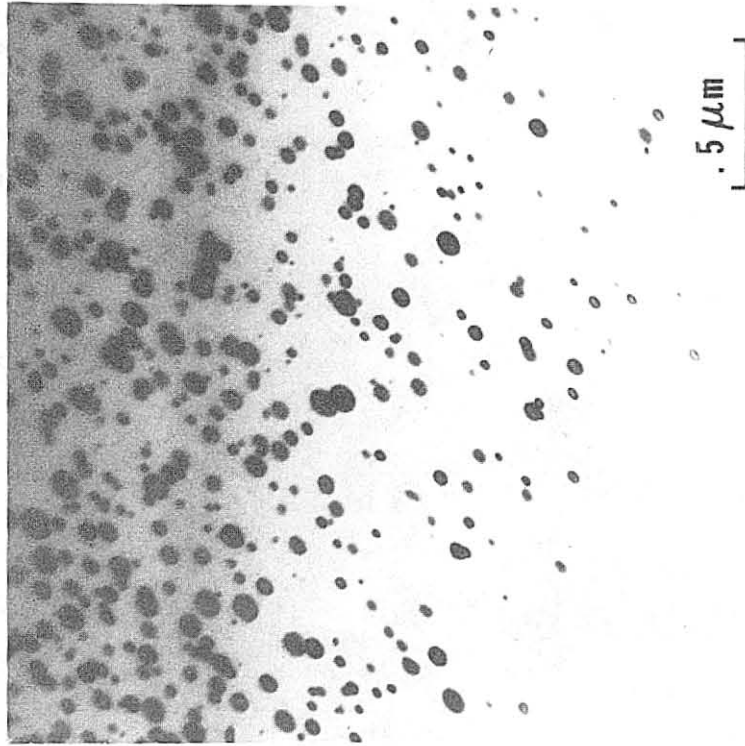


Fig. 4

XBB 827-5929



XBB 821-224

Fig. 5

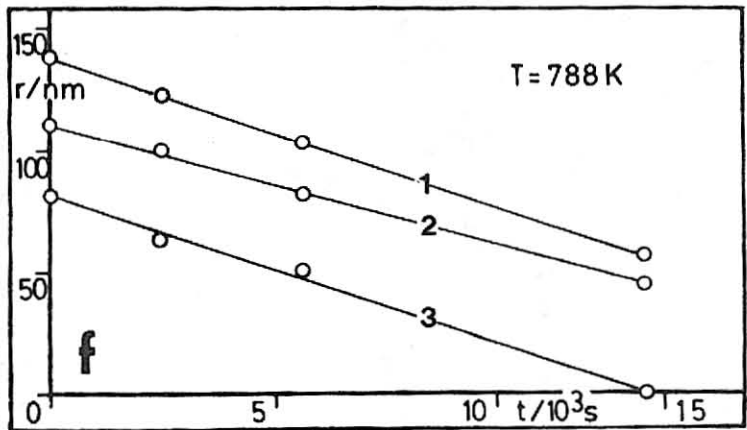
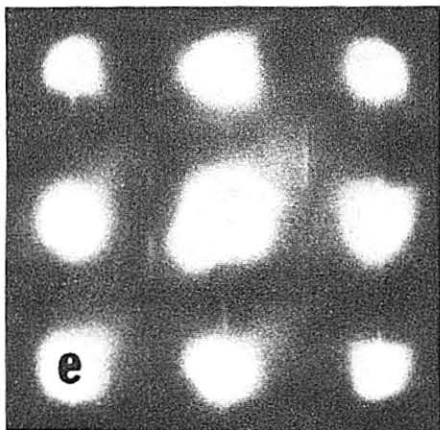
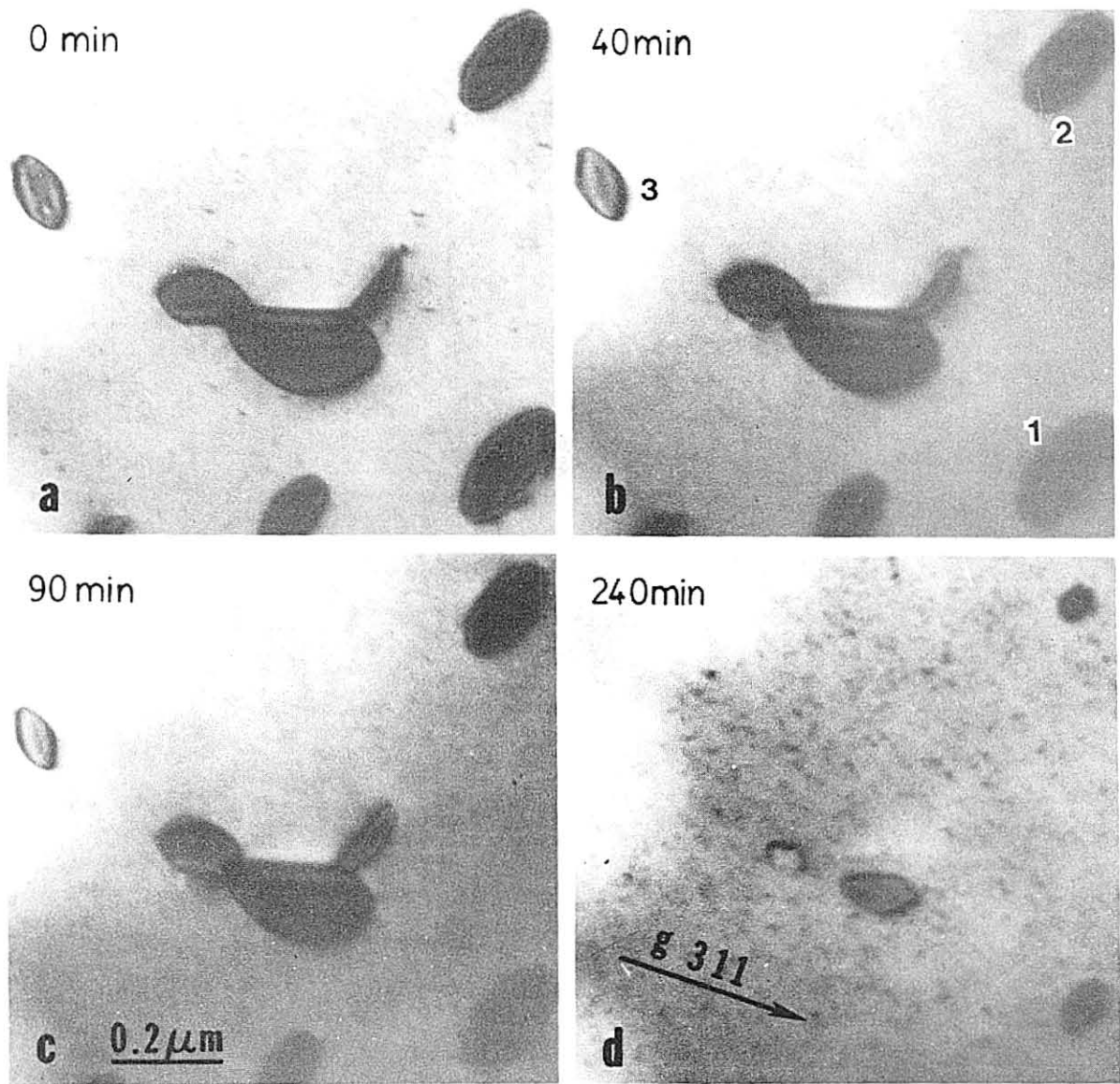


Fig. 6

XBB 827-5928

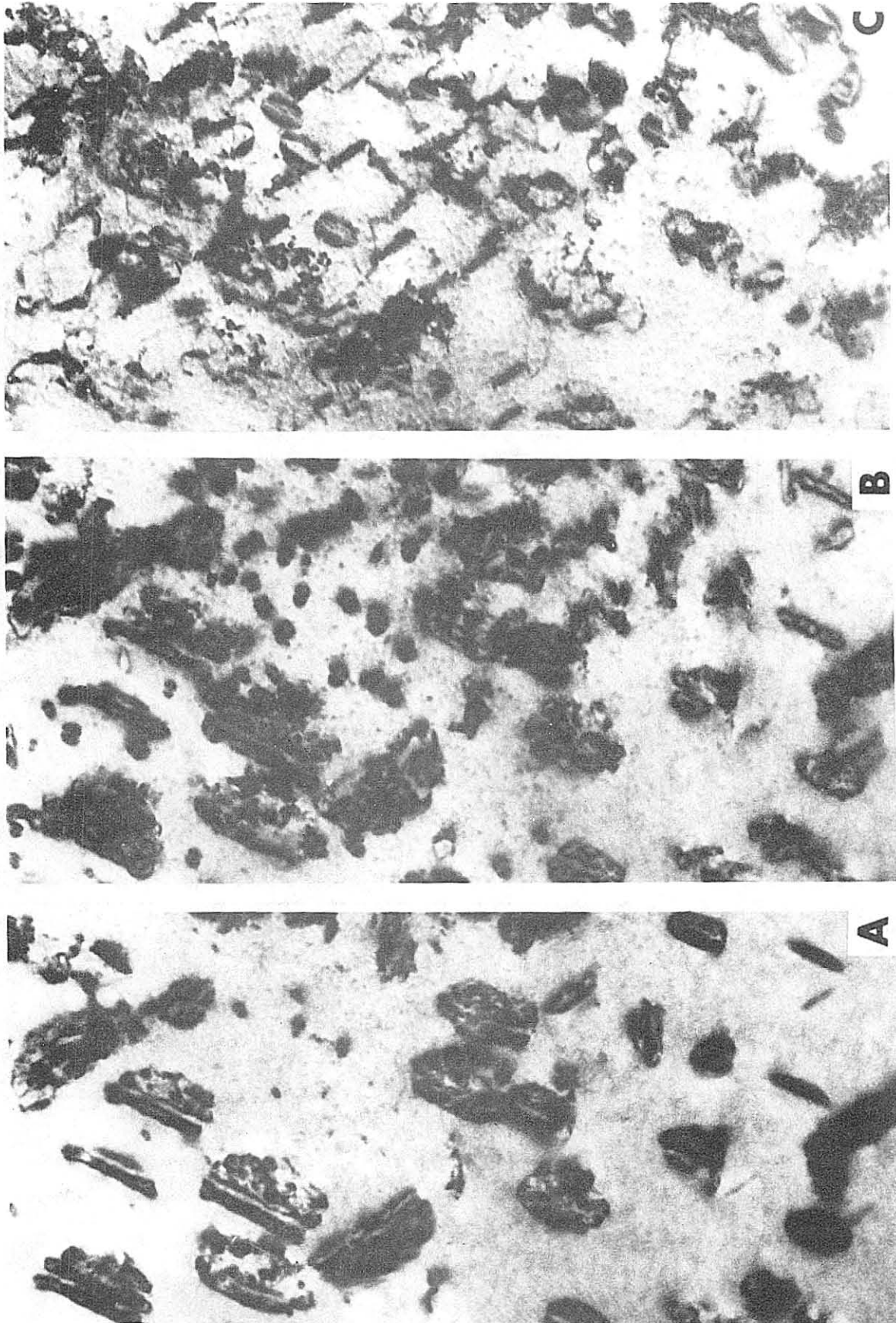
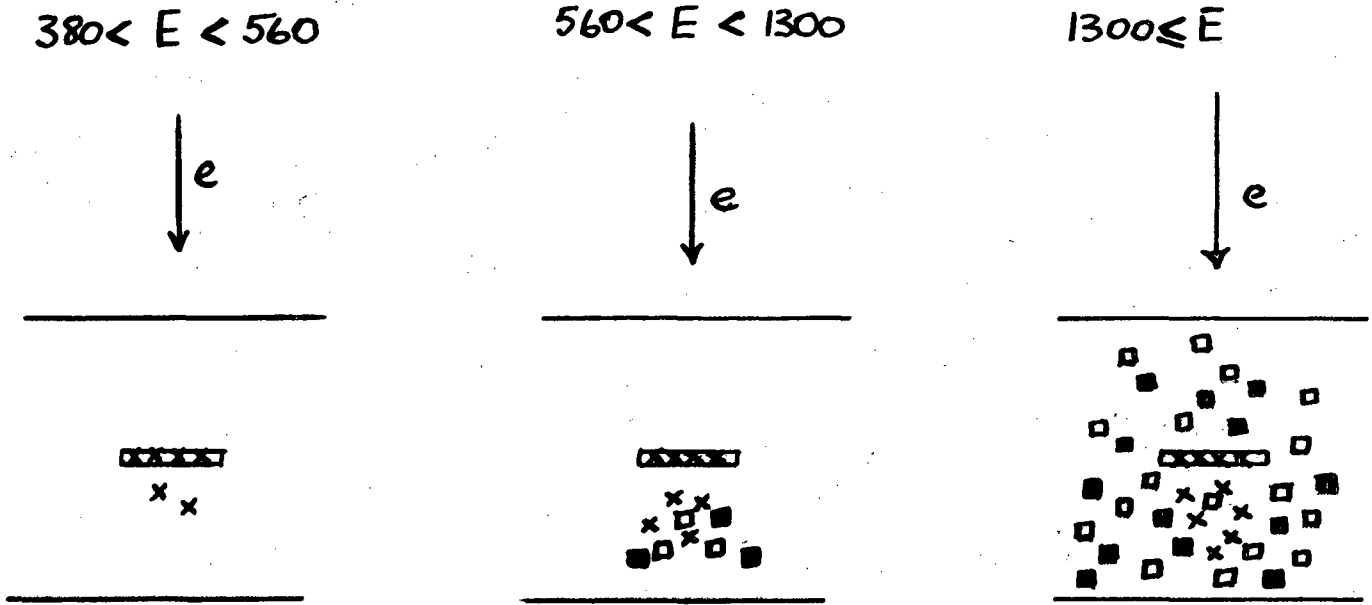


Fig. 7







- LEGEND :
-  - CARBIDE PRECIPITATE
 -  - CARBON ATOM
 -  - PLATINUM VACANCY
 -  - PLATINUM INTERSTITIAL

Fig. 8

This report was done with support from the Department of Energy. Any conclusions or opinions expressed in this report represent solely those of the author(s) and not necessarily those of The Regents of the University of California, the Lawrence Berkeley Laboratory or the Department of Energy.

Reference to a company or product name does not imply approval or recommendation of the product by the University of California or the U.S. Department of Energy to the exclusion of others that may be suitable.

TECHNICAL INFORMATION DEPARTMENT
LAWRENCE BERKELEY LABORATORY
UNIVERSITY OF CALIFORNIA
BERKELEY, CALIFORNIA 94720